

# Environmental Science Atmospheres



**Accepted Manuscript** 

This article can be cited before page numbers have been issued, to do this please use: A. M. Hurlock and D. B. Collins, *Environ. Sci.: Atmos.*, 2024, DOI: 10.1039/D3EA00142C.



This is an Accepted Manuscript, which has been through the Royal Society of Chemistry peer review process and has been accepted for publication.

Accepted Manuscripts are published online shortly after acceptance, before technical editing, formatting and proof reading. Using this free service, authors can make their results available to the community, in citable form, before we publish the edited article. We will replace this Accepted Manuscript with the edited and formatted Advance Article as soon as it is available.

You can find more information about Accepted Manuscripts in the <u>Information for Authors</u>.

Please note that technical editing may introduce minor changes to the text and/or graphics, which may alter content. The journal's standard <u>Terms & Conditions</u> and the <u>Ethical guidelines</u> still apply. In no event shall the Royal Society of Chemistry be held responsible for any errors or omissions in this Accepted Manuscript or any consequences arising from the use of any information it contains.



#### **Environmental Significance**

Thirdhand smoke (THS) – the residue and associated gases left behind by prior smoking activities – represents an important route of passive tobacco smoke exposure. Some reactions that can alter the composition and toxicity of THS have been explored, but the inherent oxidative potential of smoke suggests that oxidation reactions may occur in THS without other inputs. This study shows that THS residues become oxidized over time without added reactive gases, and that deposited cigarette smoke can oxidize co-existing films of chemicals commonly found indoors. These results suggest that surface contamination by types of particulate matter that exhibit oxidative potential could lead to transformations of surface film composition, and perhaps toxicity, that are not currently being considered.

16

17

View Article Online DOI: 10.1039/D3EA00142C

#### **ARTICLE**

## Temporal Changes in Thirdhand Cigarette Smoke Film **Composition and Oxidation of Co-existing Surface Film Chemicals**

April M. Hurlock<sup>a</sup> and Douglas B. Collins<sup>a</sup>\*

Received 00th January 20xx. Accepted 00th January 20xx

DOI: 10.1039/x0xx000000x

The composition of air-exposed surfaces can have a strong impact on air quality and chemical exposure in the indoor environment. Third hand smoke (THS), which includes surface-deposited cigarette smoke residue along with the collection of gases evolved from such residues, is becoming increasingly recognized as an important source of long-term tobacco smoke exposure. While studies have described gas/surface partitioning behaviour and some multiphase reaction systems involving THS, the possibility of time-dependent changes in chemical composition due to chemical reactivity that is endogenous to the deposited film has yet to be investigated. In this study, sidestream cigarette smoke was allowed to deposit on glass surfaces that were either clean or pre-coated with chemicals that may be oxidized by reactive oxygen species found in the smoke. Surface films included a low volatility antioxidant, tris(2-carboxyethyl)phosphine (TCEP), and two compounds relevant to surface films found within buildings, oleic acid (OA) and squalene (SQ). Upon deposition, oxidation products of nicotine, TCEP, OA, and SQ were formed over time periods of hours to weeks. The inherent oxidative potential of cigarette smoke deposited as a THS film can therefore initiate and sustain oxidation chemistry, transforming the chemical composition of surface films over long periods of time after initial smoke deposition. An interpretation of the THS oxidation results is provided in the context of other types of deposited particulate air pollutants with known oxidative potential that may be introduced to indoor environments. Continued study of THS and deposited surface films found indoors should consider the concept that chemical reservoirs found on surfaces may be reactive, that the chemical composition of indoor surface films may be time-dependent, and that the deposition of aerosol particles can act as a mechanism to initiate oxidation in surface films.

#### Introduction

Air-exposed environmental films can be formed through the deposition of organic, inorganic, and biological material for surfaces. Processes that participate in film formation generally include gas-surface partitioning,1-5 particulate matter deposition,<sup>3,5,6</sup> residue transfer by direct contact, and the application of consumer products such as cleaning agents decorative coatings, pesticides, or protective finishes.7 Th chemical composition of indoor surface films, 4,8 urban grime and other environmental films<sup>10</sup> are topics of current research as they are being recognized as important participants atmospheric and multiphase chemistry<sup>11,12</sup> and constitute important reservoirs for chemical exposure indoors.<sup>6,13,14</sup> For instance, indoor surfaces have been known to be an important sink for reactive gases<sup>15</sup> and an important source for volatile and semi-volatile organic compounds (S/VOCs). 16,17 However more recent research has characterized the dynamic chemical nature of indoor surfaces as reservoirs for bidirection 38

While the composition of a surface film may be driven, to first order, by the array of aerosol particle and SVOC sources, it may also be important to understand the role of reactivity within the film as an additional controlling factor, especially as films reside on surfaces over extended periods of time. The impact of multiphase chemistry on surfaces continues to be thoroughly studied, and many studies focus on reactive gas removal and associated chemical kinetics.7,11,12 A somewhat smaller but growing group of studies has investigated the chemical changes of the condensed phase (e.g., surface films and aerosol particles) resulting from multiphase reactions.<sup>21–24</sup> Reactive trace gases including ozone (O<sub>3</sub>)<sup>15,22,25,26</sup> and the hydroxyl radical (·OH)<sup>21,24,27</sup> have been most thoroughly investigated due to their critical roles in the multiphase oxidation of aerosol particles and interfacial films. A growing understanding of the role of autoxidation<sup>24,28,29</sup> and reactive intermediate production<sup>22,30,31</sup> in the condensed phase of multiphase chemical systems has been taking shape. The presence and persistence of reactive intermediates may lead to long-term changes in aerosol particle composition and also may lead to adverse health effects.12

Electronic Supplementary Information (ESI) available: detailed methodological information, information on control studies, and qualitative LC-MS/MS analysis. See

39

40

Ł

partitioning of compounds across a range of volatility, acidity, and octanol-air partition coefficient values. 17-20

<sup>&</sup>lt;sup>a</sup> Department of Chemistry, Bucknell University, Lewisburg, PA 17837. Email:

45

46

47

Article. Published on 05 February 2024. Downloaded on 2/5/2024 6:27:17 PM.

This article is line and the series of the s

Open Access

100

ARTICLE Journal Name

Aerosol particles have been shown to exhibit an oxidatioal potential (OP) that has been associated with negative healo2 effects. 12,32-34 In general, OP is detected and measured usio3 assays in which samples are exposed to antioxidants, the deto4 of which is then quantified. 35 Similar to the impact of oxidatio5 potential on biological systems, 36 the deposition of aeroso6 particles that exhibit OP onto surfaces may represent a mealo3 to introduce oxidants to an air-exposed surface film. Recent alo3 emerging research has been indicating that reactive oxyso9 intermediates likely form within surface films and may exhibit a persistent free radical character. 37

Deposited cigarette smoke residue and tobacco-related galas that are in pseudo-equilibrium with indoor surfaces had the collectively been termed "third-hand smoke" (THS). A loh 25 lived reservoir of cigarette smoke contaminants, THS can ac 115 a source of SVOCs, polycyclic aromatic hydrocarbons, tobact 147 specific nitrosamines, and a variety of other compounds 1168 indoor environments. 6,16,38,39 In this study, the term "THS film 19 will be used with reference to the surface-deposited fraction 120 THS material. THS is a vector for substantial environmed 21 exposures to tobacco smoke via inhalation, dermal uptake, 222 ingestion. 6,14 The magnitude of THS exposure is similar to 128 greater than second-hand smoke, with disproportionate effects on children and people with lower income levels. 40,41 Reseat 25 on THS is expanding,6 including studies of its chemis 1/2/6 physicochemical properties, exposure routes, health effeat 27 and approaches to mitigation. Specific examples of knows chemical transformations of THS residue include multipha29 reactions with nitrous acid (HONO) to form nicotine-spedi80 nitrosamines,<sup>39</sup> and the reaction of THS residue compone 131 with gaseous O<sub>3</sub>. 25,26,42 Schick and co-workers have shown that both partitioning and reactivity can occur on the 1-hb33 timescale, including the removal of several cigarette smalled components from THS films to the gas phase. Those authors also demonstrated the in situ formation of tobacco-specific nitrosamines in THS films,38 likely owing to a reaction wift HONO derived from surface uptake of ambient NO<sub>2</sub>. 136

More recent studies have probed the dynamic nature of THS in indoor environments, mainly focusing on phase partitioning processes. Components of THS, through partitioning between surfaces and the gas phase, can migrate from outdoor smoking areas to the indoors by partitioning to ambient aerosol particles that are transported by air handling systems<sup>20</sup> or by the smokers themselves. Viscosity and pH can drive chemically-selective partitioning processes to inorganic and organic aerosol particle surfaces. If the condensed phase is aqueous, it has been observed that Henry's Law can describe both uptake and office gassing, for instance from simulated lung lining fluid the supply of tobacco-related SVOCs to the gas phase over long periods of time in THS contaminated environments. In Info. 1919.

Chemical characterization of fresh cigarette smoke has been widely conducted and thoroughly documented.<sup>46</sup> While studies have sought to perform broad chemical characterizations of

THS films<sup>44</sup> and gases,<sup>16,44</sup> along with the consequences, of multiphase chemistry on THS films,<sup>25,26,39,Q2</sup> reactive processes that are endogenous to condensed-phase THS have not garnered focus. It has been known for decades that freshly collected cigarette smoke exhibits a persistent free radical character, which likely involves semiquinones associated with (mono- and poly-) aromatic compounds in cigarette smoke.<sup>47,48</sup> Radicals, reactive intermediates, and redox-active metals are associated with the induction of oxidative stress both internally<sup>47,49</sup> and externally to humans.<sup>50–52</sup>

While the OP of particulate matter is normally focused on a relationship with human health effects (via inhalation or deposition to skin), the present study explores the potential for oxidants present in the condensed phase to transform abiotic air-exposed surface films upon dry deposition, wherein the deposited particles act as an oxidant delivery vehicle. The composition, viscosity, and porosity of the substrate material has been implicated in the partitioning behaviour of compounds found in THS.<sup>44</sup> In this study, we intend to show that exposure of surfaces to sidestream cigarette smoke can induce oxidation in surface films, altering their composition to produce various oxidation products, including hydroperoxides. A non-volatile antioxidant (tris(2-carboxyethyl)phosphine; TCEP) was used to demonstrate oxidative action of THS films. Since many indoor surfaces are commonly coated with reservoirs of organic compounds, 18,53 the effect of THS film oxidation on the composition of surfaces that were pre-coated with low volatility olefinic organic compounds was also investigated. Detailed qualitative analysis of oxidized surface film proxies was conducted with an eye toward a better understanding of oxidant identity, mechanism, and time-evolving chemical exposures on THS-contaminated surfaces of increasing chemical complexity.

#### Experimental

#### **Study Design**

Sidestream cigarette smoke was generated, entrained in a sweep gas flow of ultrapure air, and then injected into a glass chamber. The chamber contained sample substrates oriented horizontally near the bottom of the chamber, resting on a glass microscope slide. After injection, the smoke was allowed to deposit on surfaces for 30 minutes before the first sample substrate was removed for analysis. To the naked eye, the optical thickness of particles in the chamber was significantly reduced during the 30-minute waiting time. Two types of experiments were conducted in the present study: (1) pooled extractions of multiple sample substrates for qualitative analysis, and (2) time-resolved experiments in which one sample substrate was extracted at a time across the period of approximately one week. In each case, triplicate measurements of each substrate extract were conducted; results are reported as the mean of replicate measurements and uncertainties reported in the study are equal to the standard deviation ( $\sigma$ ).

**ARTICLE** 

210

227

228

155 **Chemicals and Materials** 156

157

158

159

160

161

**1**62

.≇63

<del>4</del>64

₹65

**₫**66

**£67** 

**₹**68

**1**69

**₹**70

¥71

**1**72

**≟**73

**1**74

**1**75

**₹**76

**\$**77

**1**78

₹79

**9**80

**\$**81

<u>₹</u>82

**£83** 

.<u>¥</u>84

**£**85

**≇**86

.<u>1</u>87

<u> 188</u>

89

일 년 1

194

195

196 197

198

199

200

201

202

203 204

205

206

207

208

209

Downloaded on 2/5/2024 6:27:17 PM.

Article. Published on 05 February 2024.

Glass substrates were manually cut from soda-lime glass microscope slides (plain pre-cleaned; VWR Micro Slides) into 1.0 x 2.5 cm rectangles. Research cigarettes were used in the smoking apparatus (1R6F, University of Kentucky). Squalened (SQ), tris(2-carboxyethyl)phosphine (TCEP), oleic acid (OA), and bis(2-ethylhexyl)sebacate (BES) were obtained from Signation Aldrich. Acetaminophen (Sigma Aldrich) was used as a globb? internal standard. Water was obtained directly from 218 deionization system (Aries ARS-102, ResinTech, Inc.; Camde19 NJ) with a resistance of 18.2 M $\Omega$ . Formic acid (Agil**200**) Technologies), methanol (MeOH; Fisher Optima), isopropagage (IPA; BDH Analytical), and acetonitrile (ACN; Fisher Opting) were LC-MS grade. Ammonium formate (Alfa Aesar) buffer भृतृष् prepared in deionized water to a concentration of 10 mM and was then adjusted to pH = 8.5 using 6 M ammonium hydroxide solution. The background gas used in all experiments was ultra

pure air generated in the laboratory (Aadco 737-30).

#### **Sample Preparation**

229 Smoke Generation and Deposition. Smoke generation was carries out using a custom-built apparatus contained within a funget hood. The smoking protocol was adopted from the ISO smoken and smoking protocol was adopted from the ISO smoken and the ISO smoken are smoking protocol was adopted from the ISO smoken and the ISO smoken are smoken are smoken and the ISO smoken are smoken are smoken are smoken and the ISO smoken are smoken are smoken and the ISO smoken are smoken are smoken are smoken are smoken and the ISO smoken are smoken are smoken are smoken are smoken are smoken and the ISO smoken are smoke regime. A single research cigarette (1R6F; University 23B) Kentucky) was used for each experiment. The cigarette 234 manually lit with a butane lighter and placed into an aluminidas chamber for sidestream smoke delivery. Sweep gas (ultra-pare) air, 0.5 L/min) was delivered to the aluminium chamber in order to transport sidestream smoke to the 2 liter glass experime #138 chamber and also to provide oxygen for cigarette combust 1239 A diaphragm air pump and manual valve were used to gener 240 cigarette puffs for a 2 second duration every 30 seconds for 42 minutes with a flow rate of 1.5 L/min (flow rate measured w242 an acrylic variable area flow meter; Omega Engineeri Mainstream smoke was passed through a filter and the exhausted into a fume hood. Horizontally-oriented soda-life glass substrates (1 x 2.5 cm) placed near the bottom of the chamber, either clean or with an applied organic film coating, were used to collect deposited smoke. Sidestream smoke entrained in ultra-pure air was introduced to the glass experimental chamber, which was then sealed for incubation.

Organic Film Preparation. Stock solutions of SQ in ACN, BES in IPA, and OA in ACN (Chart 1) were prepared to a concentration of 9 mM and held at 4 °C until deposited on glass substrate. A  $25~\mu L$  aliquot of stock solution was deposited on each glass substrate and the solvent was allowed to evaporate under a constant flow of dry nitrogen gas.

Extraction of Samples. Sample extraction and chemical analysis was performed promptly upon removal of each substrate from the glass chamber. Substrates were removed from the glass chamber and placed directly into 20 mL scintillation vials. A 100 uL aliquot of the internal standard working solution (0.42 mg/mL acetaminophen) was added to the vial along with 900 uL of extraction solvent. For relative quantitation, of tobacco alkaloids and TCEP, the extraction solvent1034693400014400 ammonium formate buffered to pH = 8.5. For OA and SQ, the extraction solvent was a 50:50 acetonitrile/water mixture. The vial was placed on its side and extracted on an analog rocker table (VWR) for 10 mins, then the substrate was turned over and extracted for another 10 mins. Extract solution was transferred to an amber glass 2.0 mL autosampler vial (Agilent Technologies) for LC-MS analysis. Extraction efficiencies were not assessed. It is assumed that the extraction efficiency for each chemical system was consistent throughout each experiment. Absolute quantitation was not used in this study, and since all samples were normalized to the first sample in each experiment, we feel the assumption about extraction recovery is reasonable.

For qualitative analysis of reaction products in OA+BES and SQ experiments, five substrates were extracted sequentially in the same aliquot of extraction solvent to maximize film extraction into a minimal volume without the need to concentrate the samples further. Five substrates could be extracted into 2.0 mL of the appropriate extraction volume (vide supra) by placing two substrates in an extraction vial at once for 10 min on each side. Those two substrates were then removed and replaced with the remaining three substrates in the vial for 10 min on each side. All of the extraction solvent was then transferred to an autosampler vial for LC-MS analysis.

#### **Chemical Analysis**

Relative quantitation and qualitative analysis were performed using LC coupled to high resolution mass spectrometry (LC-HRMS) and/or tandem mass spectrometry (LC-MS/MS) techniques. All analytical separations were performed with reverse-phase high performance liquid chromatography using a core-shell C18 column (Kinetex C18 EVO; 100 x 3.00 mm, 5 um diameter particles; Phenomenex, Inc.) Different method parameters were used based on the desired analytes (see Table S1). A gradient method using two mobile phases was used. For the determination of tobacco alkaloids and TCEP, mobile phase

Chart 1: Compounds used to make organic surface films

250

251

252

253

254

255

**2**56

**2**57

<del>2</del>58

**2**59

**2**60

₹61

<del>2</del>62

263

₹64

**2**65

<del>2</del>66

**2**67

₹68

**≱**69

270

**Ž**71

**2**72

<u>2</u>73

**2**74

**2**75

**2**76

**Ž**77

**Ž**78

<u>2</u>79

**280** 

**2**81

**2**82

₹83

290

291

292

293

294

295

296

297

298

299

300

301

302 303

304

Downloaded on 2/5/2024 6:27:17 PM.

Article. Published on 05 February 2024.

ARTICLE Journal Name

A contained 10% methanol in 10 mM ammonium formate at 305 = 8.5, and mobile phase B contained 100% methanol. For 306 determination of OA and its oxidation products, an isocr 307 separation using 5% of aqueous 0.1% formic acid and 9398 acetonitrile was used. SQ and its oxidation products was separated with a gradient method using aqueous 0.1% for 310 acid as mobile phase A and acetonitrile as mobile phase B. 311

HRMS measurements were conducted with either an Exaction Orbitrap (Thermo Scientific) or a quadrupole/time-of-flight 304 ToF; Agilent 6560) mass spectrometer. The Orbitrap MS 345 capable of high-resolution/accurate mass acquisition of mass 6 to-charge (m/z) ratios (m/ $\Delta$ m = 60,000 at m/z 400). The Q- $3d\vec{r}$ MS was capable of a lower mass resolving power (m/ $\Delta n = 18$ 25,000 at m/z 400), but enabled tandem mass spectrometal (MS/MS) with product ion analysis that still allows for molecular formula prediction, which was used for qualitative analysis in 320 this study. Electrospray ionization (ESI) was used in all analyse except for SQ, in which atmospheric pressure chemical ionization (APCI) was implemented to enable ionization 321 analytes with lower polarity. OA and its oxidation products week analyzed in negative ion mode, but all other analyses wa? performed in positive ion mode. The Orbitrap HRMS instrum 244 was fitted with a heated electrospray ionization (Ion Max HBA) ion source and liquid handling was performed with an Access 1260 quaternary pump. Samples were manually injected in  $2\sqrt{3}$ 10 µL sample loop and separations were performed at room temperature (20-22 °C). The Q-ToF MS instrument used was capable of drift tube ion mobility measurements, but for  $\frac{378}{100}$ study it was used in "Q-ToF only" mode. The instrument 329 fitted with an Agilent Dual Jet Stream ion source for ESI and a standard Agilent APCI source for SQ experiments. Analytical separations on the LC-Q-ToF system were performed with 332 Agilent 1290 Infinity II liquid chromatograph with a quaternasy pump, automated multisampler with a variable volume loop  $\bar{351}$ to 5  $\mu$ L, and temperature-controlled column compartment held at 20 °C. See Table S2 for ion source settings for all analyses. 153 MS/MS was performed with quadrupole isolation width set 31 1.3 mass-to-charge units followed by collision induced dissociation in ultrapure  $N_2$  (Grade 5.0UH; Praxair). Further details on MS/MS settings can be found in Table S3.) 340

Standards for nicotelline, N-formylnornicotine, (S)-cotinine, 3.42 (1S', 2S')-nicotine 1'-N-oxide were obtained from Toronto 343 Research Chemicals/LGC Standards. A standard for (S)-nicotine was obtained from Cerilliant. Standards for cis-9.45 epoxyoctadecanoic acid (the epoxide of oleic acid) and 3.46 epoxidosqualene were obtained from Cayman Chemical.

#### **Data Analysis**

Qualitative analysis of Q-ToF MS and MS/MS data %50 performed with MassHunter Qualitative Analysis 10.0 (Agil§51 Technologies). Compound discovery was performed w§52 molecular feature extraction (MFE) in MassHunter, followed§58 molecular formula annotation based on comparison of measured exact mass with predicted exact mass, along with

fitting the intensities of two or more isotopologues, it can of graphical representations of data was performed with 1867 Pro 9. Relative quantitation based on Q-ToF and Orbitrap measurements was performed by directly importing raw data files into Skyline version 22,54,55 wherein extracted chromatographic peaks were integrated and normalized to the internal standard. Time series experiments were quantified on a relative basis using triplicate LC-MS injections of each sample that was extracted at different incubation times in the glass chamber. For each sample extracted at time point (t), the peak area (A) for each compound (j) was first normalized to the peak area of the internal standard (IS) for each repeated measurement (i). The normalized areas were then averaged over the total number of repeat injections (n) to obtain an averaged, IS-normalized signal (S<sub>j,t</sub>).

$$S_{j,t} = \frac{1}{n} \sum_{i=0}^{n} \binom{A_{j,t,i}}{IS_{t,i}}$$
 (1)

In temporal experiments, to obtain a relative amount of change in the abundance of each compound, the average, IS-normalized signal  $(S_{j,t})$  was divided by the same metric at the first time point  $(S_{j,t=0})$ , which has been assigned t=0 h (but truly was exposed to the inside of the chamber for 30 mins while smoke was depositing). Therefore, the relevant quantity shown in temporal analysis figures amounts to a 'fold change' metric.

#### **Results and Discussion**

#### **Chemical Transformations of THS Films on Clean Glass**

THS films were generated via dry deposition of sidestream cigarette smoke. An initial suspect screening analysis was conducted using HRMS measurements of THS film extracts from clean glass surfaces. Exact mass matches to molecular formulae (with support from two or more stable isotopologues) with mass accuracy better than 5 ppm were obtained for a list of 12 tobacco-related compounds listed in Table S4. Most of the matched exact masses had extracted ion chromatograms exhibiting a single chromatographic peak. Such was the case for m/z 161.1079, although several isomeric compounds with the molecular formula  $C_{10}H_{12}N_2$  (computed m/z = 161.1073 [M+H]<sup>+</sup>) are known to be found in tobacco smoke. Two sets of isobaric, but chromatographically separable compounds were observed: one pair of chromatographic peaks with m/z 177.1026 and another pair with m/z 179.1181. Tandem MS analysis enabled assignment of cotinine and N-formylnornicotine to each of the chromatographic peaks that appear in the extracted ion chromatogram for m/z 177.1026 (Figure S3). The MS/MS spectra for the two chromatographic peaks with m/z 179.1181 exhibited high similarity (Figure S4) and corresponded with the detailed ESI-MS/MS studies of nicotine oxides by Smyth et al.,56 suggesting that a pair of nicotine 1'-N-oxide diastereomers were formed and detected.

nospheres Accepted Manus

**ARTICLE** 

75

**7**6

77

18

19

30

31

32

33

34

35

36 37

38

39

10

1(

12

)3

)4

95

16

17

18

99

)0

)1

12

**4U3** 

421

nicotine 1'-N-oxides

nicotelline

mz147

mz157

mz161

100

120

N-formylnornicotine

nicotine

mz193

mz240

140

160

**Journal Name** 

100

80

60

40

20

2.5

2.0

1.5

1.0

0.5

0.0

8.0

0.4

0.0

0

20

40

60

triplicate LC-HRMS injections. Replicate experiments are shown in Figure S5.

80

Figure 1: Time series of compounds listed in Table S4 grouped by observed behaviour in THS film extracts. Species are labelled with a chemical name if they have been verified.

beyond exact mass and stable isotope matching. Compounds that increased in;

abundance are shown in (A), those that were consistent during the experiment are

shown in (B), and those that decreased in abundance are shown in (C). The substrate was

clean glass. A dashed back line is shown at where  $S_{j,t} / S_{j,t=0} = 1$  on each vertical axis. All panels share a horizontal time axis. Error bars represent the standard deviation of

Several of the compounds in Table S4 were removed from #140

THS film over time relative to the t = 0 sample. Four of 414

matched suspect compounds had consistent relative signal

levels throughout one week of aging under whole sidestreah

cigarette smoke. As noted above, MS/MS experiments supplif

putative annotations of the four compounds in Figure 18435

cotinine (mz177a), N-formylnornicotine (mz177b), nicotel

(mz234), and nornicotine (mz149). Removal of nornicotine 43

observed in some replicates and to some degree between 14918

and 167.5 hours in the experiment depicted in Figure 1, 4110

perhaps could be grouped with compounds shown in panel \$20

Some compounds were removed during the study period while

others were steady in abundance relative to a sample collected

approximately 30 minutes after smoke generation (Figure 1).

Nicotine was the most readily observed compound in the

sample and decreased by at least80% after 150 hours across all

experimental replicates. It is possible that evaporative losses

could contribute to the decreasing trend in nicotine and other

SVOCs. However, the appearance of nicotine 1'-N-oxides

provided evidence that nicotine removal was at least partially

Aging Time (h)

Sjt / Sjt=0

Δ

mz149

cotinine

373 374

368

369

370

371

372

This journal is © The Royal Society of Chemistry 20xx

## the extent of removal via film-to-gas partitioning would not be as important as for a film bathed in ventilated (nicotine-poor) air. The total mass of nicotine in the chamber (surface-sorbed + gaseous) should be largely consistent across the entirety of the In a more detailed temporal trend analysis, focus will be placed nicotelline, and the sum of both nicotine 1'-N-oxide

due to oxidation. The earlier-eluting diastereomer had a smaller

peak area than the later peak and the relative ବର୍ଣ୍ଟେ ଅନ୍ୟାନ୍ତ ନର୍ମଣ ନର୍ମଣ ବର୍ଷ

the earlier peak was greater than for the later-eluting nicotine

oxide peak (Figure 1A). Removal of nicotine from the film via

partitioning to the gas phase was not out of the question;

however, the samples were incubated under whole smoke so

on the behaviour of nicotine, N-formylnornicotine, cotinine, diastereomers (Chart 2). MS/MS data for each compound in Chart 2 has been verified against an authentic standard (Figures S3 and S4). Nicotelline has been identified as a reliable tracer for tobacco smoke and THS,57,58 and in this study it provided a measure of consistency between samples in each experiment. In the present study, cotinine and N-formylnornicotine exhibited different behaviour depending on the conditions of the surface onto which smoke was deposited. On clean glass, cotinine and N-formylnornicotine were largely unchanged in relative abundance through 170 hours of incubation (Figure 1B), despite the fact that both have been demonstrated as products of nicotine oxidation.42,59

THS Deposition on a Low-Volatility Organic Antioxidant Film Demonstration of Film Oxidation upon Smoke Deposition. In order to clearly demonstrate the potential for dry deposited smoke to act as an oxidant on surfaces, a film of a low-volatility tris(2-carboxyethyl)phosphine (TCEP, antioxidant, 251.0679 [M+H]+), was applied to glass substrates prior to smoke exposure and deposition. Formation of TCEP oxide was monitored at m/z 267.0628 [M+H]+. Figure 2 shows the temporal profile of nicotine, the sum of both nicotine oxide isomers, TCEP, and TCEP oxide on a glass surface. TCEP was removed from the surface film and a corresponding signal for TCEP oxide was observed. Control experiments showed that TCEP was not oxidized or removed from surface films under zero air during comparable timeframes (Figure S8), so the removal of TCEP can be attributed to sidestream cigarette

Nicotine oxide formation was observed coincident with TCEP oxide formation, indicating that TCEP did not fully quench the

Chart 2: Main tobacco alkaloid target compounds

smoke exposure within the chamber.

nicotelline

423

424

425

426 427

428

429

**₫**30

**₫**31

**4**32

**4**33

434 435

**4**36

₹37

**4**38

**₫**39

**₫**40

**₫**41

事42

**4**43

**4**44

**4**45

<u>4</u>46

447

448

**4**49

₫50

**4**51

<u>¥</u>52

**4**53

**₹**54

455

**₽**56

Downloaded on 2/5/2024 6:27:17 PM.

Article. Published on 05 February 2024.

Open Access

ARTICLE Journal Name

oxidative capacity of the deposited smoke. It is also possible that deposition was locally inhomogeneous on the TCEP surface film, precluding TCEP from mixing with and quenching oxidants in every deposited particle, or perhaps even across the entire mass of an individual deposited particle. For instance, when considering the deposition of an individual smoke particle onto a TCEP film, it may be that oxidants near the surface of the particle – at the TCEP/particle interface – proceeded to oxidize the antioxidant probe, but material buried more deeply within individual particles still reacted with abundant reduced organic compounds that are characteristic of the smoke sample itself, of which nicotine is an especially abundant example.

Contribution of SVOC Partitioning to TCEP Films. First, it should be noted that the experimental apparatus was not designed with SVOC partitioning studies principally in mind and is not optimized for such experiments. However, interpretation of some of the time series data benefits greatly from, or even requires, consideration of partitioning behaviour, so a limited discussion of the issue is provided here. Interestingly, the signal for nicotine increased during TCEP experiments (Figure 2), along with increases in the abundance of cotinine and Nformylnornicotine (Figure 3). The increase of nicotine coincided with the formation of nicotine oxides, which rose in abundance more quickly than on clean glass. It is possible that the nicotine was taken up from the gas phase into the TCEP film, also leading to increased production of nicotine oxidation products (nicotine 1'-N-oxides, cotinine, N-formylnornicotine). Since cotinine and N-formylnornicotine were present in freshly emitted sidestream smoke (present in all t=0 samples), their increasing trends could contain a contribution from SVOC partitioning. similar to the proposed process involving nicotine. To probe this possibility, a comparison with other SVOCs detected in THS fills extracts was conducted. The smoke-contaminated chamber walls can act as a source of SVOCs during the experiment (the same as a smoke-contaminated indoor environment), 465

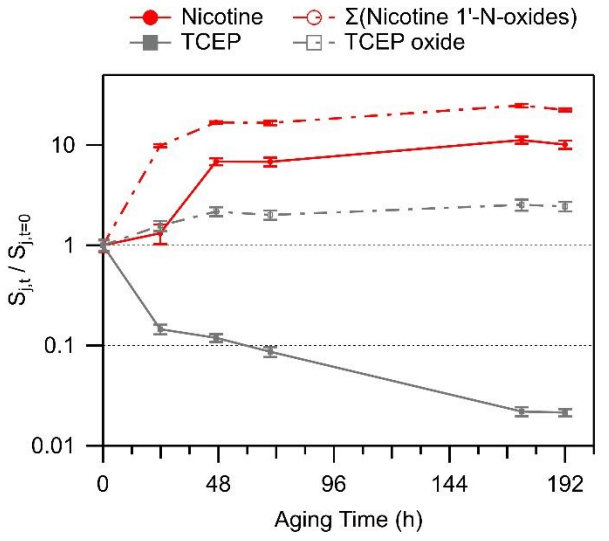
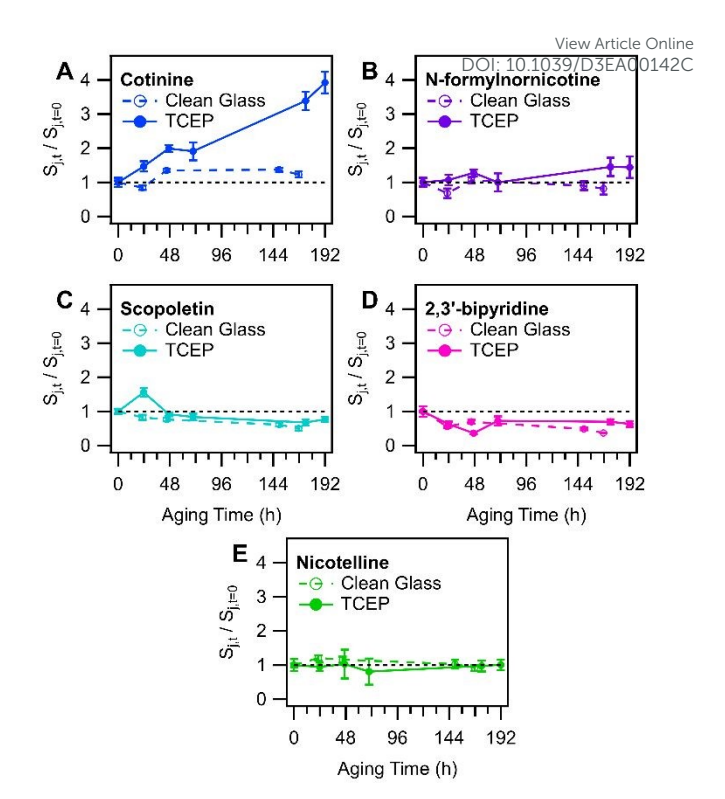


Figure 2: Temporal changes in nicotine, nicotine 1'-N-oxides (sum of diastereomers), TCEP, and TCEP oxide. Values above unity indicate an increase in abundance on the glass substrates, while values less than unity indicate net removal. Error bars represent one; standard deviation based on triplicate LC-HRMS injections. Experimental replicates are; shown in Figure S9.



**Figure 3**: Comparison of temporal profiles of tobacco-related compounds extracted from clean glass substrates versus glass substrates (in a separate experiment) that were coated with TCEP before exposure to tobacco smoke. Error bars represent one standard deviation based on triplicate LC-HRMS injections of each sample.

sufficiently volatile compounds can dynamically repartition to and accumulate within the TCEP film from the chamber walls. The TCEP film could be envisaged as a 10-20 nm thick film of viscous organic material; slow mass transport within the film may contribute to a prolonged uptake of nicotine, beyond what is delivered via smoke particle deposition. Nicotelline, which did not change in abundance over time in either the clean glass (Figure 1B) or TCEP cases (Figure 3E), has an octanol-air partition coefficient (log Koa = 13.5) that is approximately 260,000 times larger than that of nicotine (log  $K_{oa}$  = 8.08;  $K_{oa}$ values were predicted using KOAWIN, EpiSuite, US EPA). Its equilibrium gas-phase mixing ratio would be much smaller than that of nicotine, cotinine, and N-formylnornicotine (if each compound was in equal abundance), so the potential for repartitioning from deposited smoke found elsewhere in the chamber to the TCEP film was expected to be minimal. The significantly lower volatility of nicotelline allows for the attribution of a vast majority of its signal to direct aerosol particle dry deposition, while abundances of nicotine, cotinine, and N-formylnornicotine (and other alkaloids with similar volatilities) may be more substantially influenced by SVOC partitioning. To further investigate the strength of SVOC partitioning to the TCEP film, the behaviour of cotinine (log Koa = 9.93) and N-formylnornicotine (log K<sub>oa</sub> = 9.98) was compared with two other SVOCs that have similar  $K_{oa}$ . Scopoletin (log  $K_{oa}$ = 9.62) and 2,3'-bipyridine (log  $K_{oa}$  = 8.99) both decreased slightly in abundance in film extracts of TCEP-coated glass substrates, while cotinine and N-formylnornicotine showed relative increases in abundance in the same extracts (especially

)

3

i

Journal Name ARTICLE

cotinine; Figure 3). The relationships between the measured compounds therefore suggest that nicotine oxidation was an important contributor to the increasing trends in cotinine and N-formylnornicotine on TCEP films. It was interesting that nicotine oxidation continued to produce nicotine 1'-N-oxide, cotinine, and N-formylnornicotine in the presence of TCEP due to the reducing environment of the film. Localization of oxidation chemistry within deposited particulate matter that is not in direct contact with the solid TCEP coating is a tempting explanation. However, such an explanation would seem to necessitate a similar type of observation in extracts from clean glass, wherein the relative abundances of cotinine and N-formylnornicotine were *not* observed to increase.

487

488

489

490

491

492

493

494

₹95

<del>4</del>96

**4**97

**4**98

**4**99

₩00

\$01

₹02

**₹**03

₹04

\$05

5€06

₹07

508

₹09

§10 §11

**§**12

517 518

₹19

<u>5</u>20

!3

6

528

529

530

531

532

533

534

535

536

537

538

539 540

541

542

Den Access

Article. Published on 05 February 2024. Downloaded on 2/5/2024 6:27:17 PM.

#### **Effects of Cigarette Smoke on Organic Surface Film Composition**

In order to investigate the chemical outcomes of THS mixing with other organic film-forming materials on indoor surfaces, a series of trial films were deposited on glass and exposed to sidestream cigarette smoke, just as in the clean glass and TCEP cases. Three compounds, in addition to TCEP (Chart 2), were tested as films: a weakly-reactive oil (bis(2-ethylhexyl)sebacate; BES), a monounsaturated fatty acid (oleic acid; OA), and a polyisoprenoid (squalene; SQ). Since OA did not deposit evenly on the surface by itself, it was co-deposited with BES. The two compounds were deposited successively: BES followed by OA.

Bis(2-ethylhexyl)sebacate (BES). Based on prior multiphase oxidation studies, <sup>60</sup> BES was expected to have low reactivity and was included in the study primarily as a vehicle for oleic acid **6443** formation. <sup>61</sup> BES did not form a monolayer (or 'flat' multila **544** film on glass – rather it formed an array of beads or small dr **545** as observed by other investigators. <sup>61</sup> Still, BES is a useful **546** case as a low-viscosity, low-reactivity organic surface **5467** reservoir for deposited THS.

Upon exposure to smoke and subsequent incubation, nico 550 oxide formation was observed in BES film extracts, just a551 experiments with other surface films (and on clean glass), 552 changes in nicotine, cotinine, and 553 formylnornicotine abundance were most similar to clean g554 (Figure S10). The lack of observable uptake of nicotine to 555 on the multi-day timescale may be related to rapid equilibra 556 with the low-viscosity film material. If gas-film SVOC equilibr 5.57 was largely complete by the time the first sample was collected. and extracted, approximately 30 minutes after smoke was 559 introduced to the glass chamber, the trend in nicotine would 160 normalized after equilibration occurred. The results of 561 experiments, considered in concert with TCEP experim 562 results, suggest the importance of kinetic limitations to SV563 partitioning (slow diffusion and gradient formation)8,19,6564 viscous organic films, along with the participation of the film 65 theformation of reactive species or intermediates.

**Oleic acid.** THS deposition on mixed OA/BES films showed a prompt removal of OA, with concomitant formation of oxidized products consistent with the addition of one or two oxygen

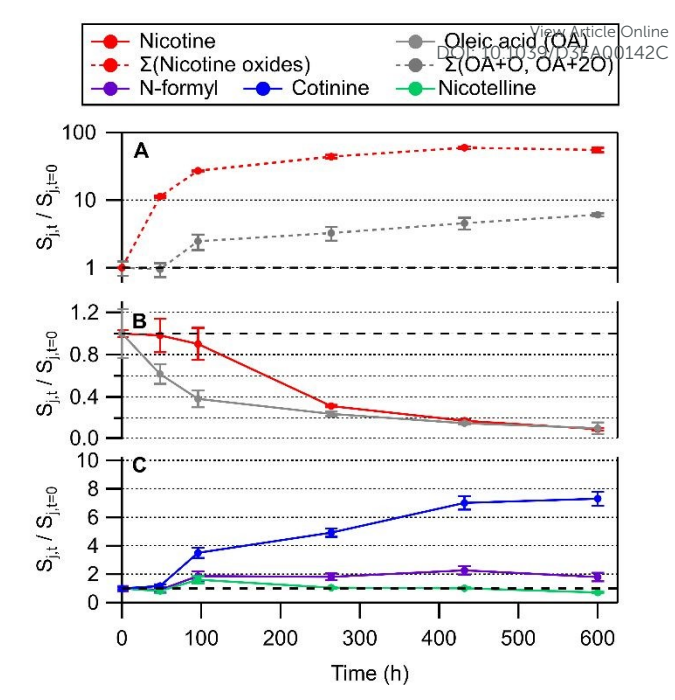


Figure 4: Time series of chemical transformations in an OA/BES film upon cigarette smoke deposition, including (A) nicotine oxides and TCEP oxide, (B) nicotine and oleic acid, and (C) other tobacco related alkaloids. Panel (A) is shown with a logarithmic axis to display a wide degree of change in relative abundance in oxidation products. Oxidation product traces represent the sum of nicotine 1'-N-oxide diastereomers ( $\Sigma$ (Nicotine oxides)) and the sum of all peak areas from OA+O and OA+2O ( $\Sigma$ (OA+O, OA+2O)). OA+O and OA+2O are shown in detail in Figure 5. Error bars represent the standard deviation of three repeat injections.

atoms to OA. Removal of nicotine and production of nicotine 1'-N-oxides was observed, along with the formation of cotinine and N-formylnornicotine (Figure 4). A longer experiment time (600 h) was used for THS interactions with OA/BES film to accumulate a greater mass of oxidation products for HRMS studies. Most of the change in the sum of OA oxidation products occurred within approximately 100 h of incubation time (Figure 4A), despite more consistent formation of certain (less abundant) oxidation products over the whole 600 h experiment timeline (Figure 5D and E). A delay in the removal of nicotine was observed, which may be associated with a combination of reactive decay and re-supply to the organic film via gas-to-film partitioning. A pronounced increase in cotinine was associated with the removal of nicotine over the course of the experiment; a similar rate of increase was observed in TCEP+THS experiments. N-formylnornicotine was formed to a lesser extent relative to the t = 0 h sample, which was also consistent with TCEP experiments. The pronounced formation of nicotine oxidation products in the (OA/BES)+THS test case (Figure 4A and C) compared with the BES+THS case suggested that the formation of reactive intermediates from OA oxidation may have been involved in the formation of cotinine and Nformylnornicotine.

568

569

570

571

572

573

574

**§**75

**5**76

§77

**₽**78

**5**79

580 581

**§**82

₫83

**£**84

<u>5</u>85

<u>\$</u>86

**5**87

**588** 

**Š**89

<del>5</del>90

<u>\$</u>91

**₹**92

**5**93

₹94

**5**95

**§**96

<u>\$</u>97

<del>5</del>98

399

600

€01

12

**)**5

608

609

610

611

612

613

614

615

616

617

618 619

620

621

622

623

Open Access

Article. Published on 05 February 2024. Downloaded on 2/5/2024 6:27:17 PM.

Journal Name

Qualitative analysis of LC-HRMS data for THS + OA extracts 624 processed with non-targeted molecular feature extraction us 25 MassHunter. Several chromatographically separable oxidat626 products of OA were observed in LC-HRMS measurements v627 negative-mode ESI. Three chromatographic peaks (labelled 1628) and 3 in Figure 5B) were observed in the extracted 6229 chromatogram (EIC) for m/z 297.2438 [C<sub>18</sub>H<sub>34</sub>O<sub>3</sub>-H]<sup>-</sup> and **to**20 peaks (labelled 4 and 5 in Figure 5C) were observed in the 631 for m/z 295.2280 [C<sub>18</sub>H<sub>34</sub>O<sub>4</sub>-H<sub>2</sub>O-H]<sup>-</sup>. Measured stable isot **632** abundance ratios were compared with computed isot 638 abundances using the idotp metric (a vector-based simila634 metric having a scale similar to a dot product) in Skyline. 835 Molecular formulas reported had idotp values greater than 6.36 which support the molecular formula assignments for both  $[C_{18}H_{34}O_4-H_2O-H]^-$  and  $[C_{18}H_{34}O_3-H]^-$  across all chromatographic peaks shown in panels B and C in Figure 5. While some chromatographic peaks associated with OA+O and OA+2O overlap to some degree, retention times identified at peak centroids differ at least slightly (Table S5). None of the chromatographic peaks of interest for m/z 295.2280 or m/z 297.2438 co-eluted with the OA starting material (m/z 281.2488 [C<sub>18</sub>H<sub>34</sub>O<sub>2</sub>-H]<sup>-</sup>; Figure 5A) nor did they perfectly co-elute with one another. Therefore, in-source oxidation, fragmentation, and other possible ion chemistry artefacts involving the starting material were likely not a factor associated with the observation of OA+O or OA+2O features by LC-HRMS.

The formation of  $C_{18}H_{34}O_3$  compounds based on the addition of a single oxygen atom to oleic acid (OA+O) may include oleic acid epoxide, ketostearic acid, or hydroxyoleic acid. Indeed, three chromatographic peaks appear in the EIC for m/z 297.2438 (Figure 5B). Peak 1 was the largest OA+O signal throughout the experiment and also increased the most overall, while Peaks 2 and 3 increased for approximately 100 h and then were stable or showed a decrease in area (Figure 5D). Measurement of an OA epoxide standard produced a single chromatographic peak at 1.64 min, overlapping well with Peak 2 (Figure S11). Collisioninduced dissociation of the chromatographically-resolved oxidized OA precursor ions was not successful, so further structural characterization was not possible for OA oxidation products. Still we speculate that OA+O Peaks 1 and 3 may correspond with molecules such as ketostearic acid and/or hydroxyoleic acid.

When OA/BES films were incubated under ultra-pure air (see Supplementary Information), the formation of OA+2O signals were similar in magnitude and temporal trend to signals observed in the THS treatment so Peaks 4 and 5 will not be discussed in greater detail. It is worthwhile to note that OA+2O species would be expected to form on air-exposed surfaces in indoor environments.

**Squalene.** Analysis of chemical changes upon exposure of SQ films to sidestream cigarette smoke will be restricted to product analysis of SQ oxidation. A temporal analysis of tobacco alkaloids was not possible due to poor extraction efficiency from the squalene film. A clear signal for unreacted SQ was

observed in sample extracts (Figure 6), along with Afeatures corresponding to two SQ oxidation products wherein Added of two oxygens were incorporated into squalene, respectively (SQ+O and SQ+2O). Both compounds also exhibited signal intensity as a co-elution with SQ, indicating that oxidation of SQ in the APCI source was occurring. However, a shift of all oxidation products to earlier retention times in the chromatogram (compared to SQ) provides evidence that the features identified as SQ+O and SQ+2O were indeed more polar than SQ, and were oxidized prior to analysis, so instrumental artifacts can be ruled out for oxidized SQ signals except those that co-elute exactly with SQ (Figure 6).

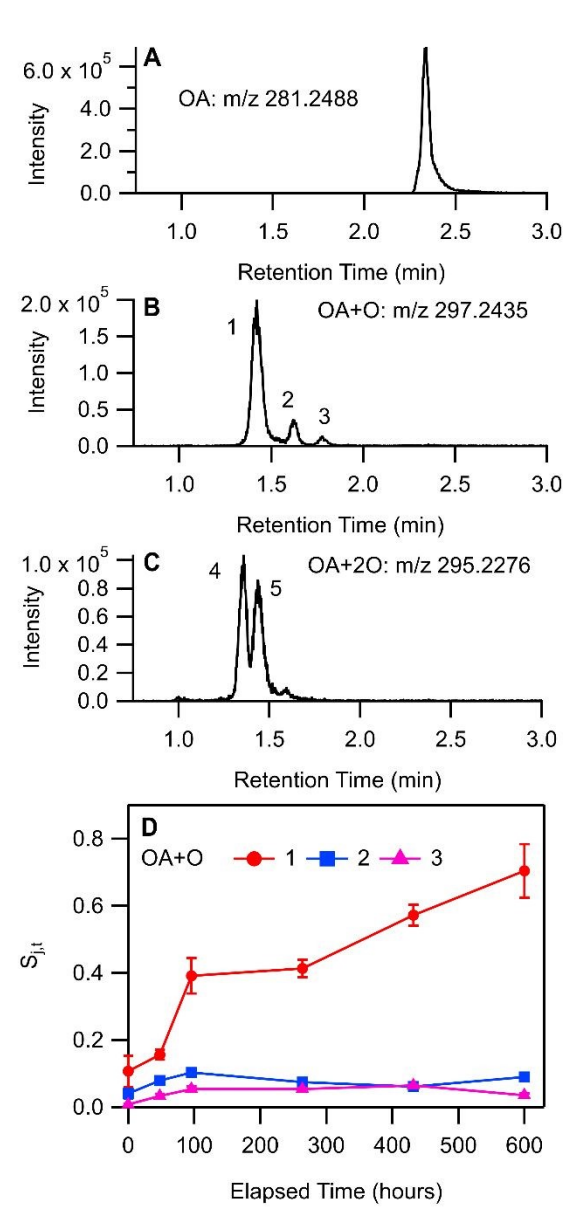


**Figure 5:** LC-HRMS product analysis of OA/BES reaction with deposited THS. Chromatograms from the 600 h sample for (A) oleic acid, and its oxidation products (B) OA+O and (C) OA+2O, represented by the extracted ion chromatograms for mass-to-charge ratios shown. Panel (D) shows the mean of internal standard-normalized areas of chromatographic peaks labelled in panels (B) and (C). Error bars in (D) represent the standard deviation of three repeat LC-MS injections.

638

639

640

641

642

643

644

€45

£46

647

**6**48

**6**49

€50

651

₫52

**6**53

£54

**6**55

<u>€</u>56

₿57

**6**58

€59

660

<u>6</u>61

662

€63

₿64

₫65

666

<u>6</u>67

668

€69

670

**6**71

2

**'**5

6

678

679

680

681

682

683

684

685

686

687

688

689

690

691

692

693

Open Access

Article. Published on 05 February 2024. Downloaded on 2/5/2024 6:27:17 PM.

ARTICLE

Molecular formula and adduct assignments for LC-HR6994 features in Figure 6 were supported by comparing calcula 695 and measured peak area ratios of the three most abund 696 isotopologues using the *idotp* function in Skyline;54,55 signed 3 obtained each chromatographic peak found in an EIC had id 698 > 0.9. Oxidation of SQ leading to the addition of a single O atomo suggests the formation of SQ monoepoxide, similar to OA. The MS and MS/MS spectra were consistent with prior reports of epoxide detection, 63,64 and the SQ+O signal from a THS+ sample collected at 216 h of incubation was a close match the SQ epoxide standard (Figure S17). The presence of a single chromatographic peak in the EIC for m/z 427.3935 (labelled 1/1) Figure 6B) was somewhat surprising given the variety786 possible SQ+O isomers, although based on prior studies,63,65,05 is likely that reverse phase liquid chromatography may not be capable of resolving isomers of SQ+O.

The detection of SQ+2O compounds occurred consistently as a proton adduct with a neutral loss of H<sub>2</sub>O [M+H-H<sub>2</sub>O]<sup>+</sup> (m/z 425.3779), the EIC of which shows at least three chromatographic peaks (labelled 2, 3, and 4 in Figure 6C). Other related ions were detected in MS1 spectra collected for peaks 2and 3 (Figure S16, Table S7), including a small signal at m/z 443.3890 [C<sub>30</sub>H<sub>50</sub>O<sub>2</sub>+H]<sup>+</sup> which corresponded with intact, protonated SQ+2O. Neutral loss of H<sub>2</sub>O from SQ+2O<sup>65,66</sup> along with the likelihood of free radical-initiated autoxidation may suggest the existence of a SQ hydroperoxide (SQ-OOH) in the sample extracts, although other oxygenated functional groups are possible. MS/MS spectra for m/z 425 were used to gain further insight into the structural similarities and differences between molecules eluting in peaks 2, 3, and 4 (Figure S18). Further loss of H<sub>2</sub>O to form a fragment at m/z 407.3812 was observed in all three MS/MS spectra. Peaks 2 and 4 show an MS/MS fragment at m/z 339.3034, a close exact mass match (3.6 ppm) to the  $[C_{25}H_{38}+H]^+$  ion, which corresponds to the collision-induced loss of one isoprene unit and an oxygen atom. The MS1 spectra for Peaks 2 and 4 were also similar, with m/z 425.3779 and m/z 407.3678 as the most prominent features, which bear striking similarity to MS1 spectra for SQ-OOH substituted at odd-numbered positions as reported by Shimizu et al.<sup>67</sup> Peak 3 has a somewhat different MS/MS spectrum and a markedly different MS1 spectrum compared to Peaks 2 and 4. In-source fragmentation was a prominent feature of the Peak 3 MS1 spectrum (Figure S16), suggesting a relatively labile SQ+20 species. Among the prominent signals in the MS1 spectrum of Peak 3 were in-source fragments m/z 425.3779 from the neutral loss of H<sub>2</sub>O from SQ+2O, and also m/z 411.3629 from the neutral loss of CH<sub>3</sub>OH from SQ+2O (a more detailed dissection of the data is provided in Section S7 of the Supporting Information). The MS/MS spectrum for Peak 3 contained a signal at m/z 269.2263, which corresponded to only four contiguous isoprene monomer units of SQ (loss of two 5-carbon subunits). Taken together, the two different neutral losses from SQ+2O along with the MS/MS observation of the loss of two 5carbon subunits from SQ+2O suggest the oxidation of SQ at two different olefinic sites, perhaps at either terminus of the SQ chain (the 2/3 and 22/23 positions). Assignment of the

compound that eluted at Peak 3 to SQ-OOH is therefore pot so compelling and may instead arise from an SQ120/product an which two separate hydroxyl or carbonyl groups are present. 68

#### Insights on the Nature of Endogenous Oxidation in THS Films

Tobacco smoke aerosol is known to contain iron, so Fenton chemistry is often implicated in reactions leading to smoke-related oxidative stress.<sup>34</sup> While the active reactive oxygen species (ROS) were likely OH and HO<sub>2</sub> radicals, longer-lived aromatic and polycyclic aromatic semiquinones in cigarette smoke 'tar' are thought to sustain the oxidative potential of tobacco smoke<sup>34,47,49</sup> and are notable as environmentally persistent free radicals (EPFRs). Based on the literature, along with oxidation product analysis of SQ and OA film oxidation by

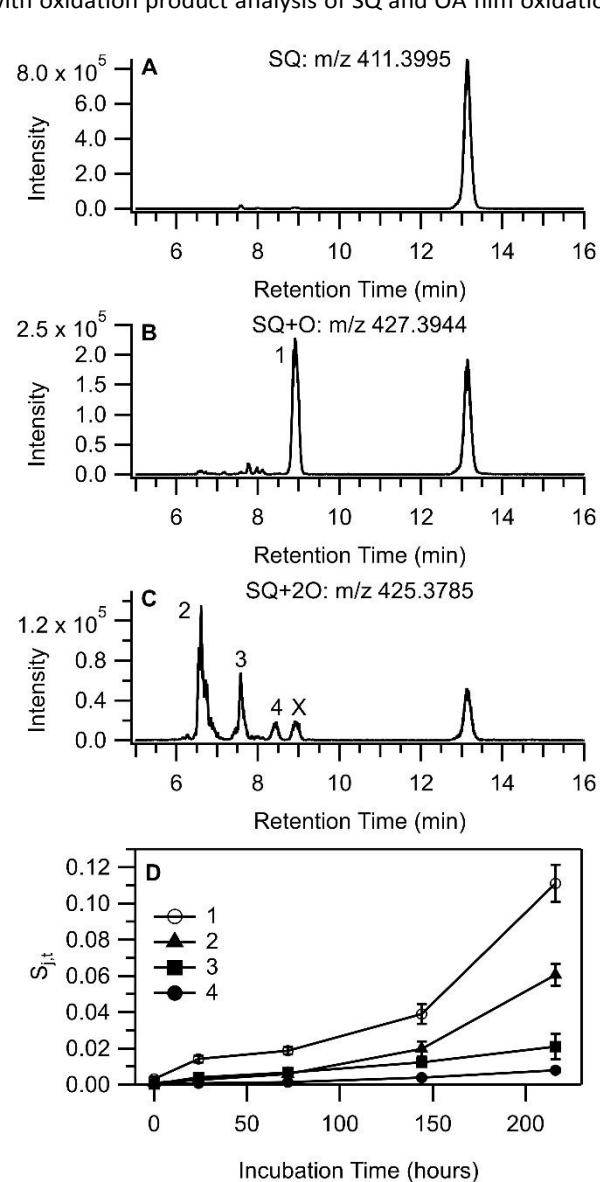


**Figure 6:** LC-HRMS product analysis of SQ reaction with THS residue. Extracted ion chromatograms from the sample incubated for 216 h corresponding to (A) SQ, (B) SQ+O, and (C) SQ+2O are shown. The peak labelled "X" in (C) overlaps exactly with peak 1 and was not considered further. Intensities are the sum of the three most abundant isotopologues. Panel (D) shows the temporal profile of SQ+O and SQ+2O peak area (after internal standard normalization). Chromatographic peaks labelled with numerals in (B) and (C) match with legend entries in (D).

708

709

710

711

712

713

714

**7**15

₹16

<del>7</del>17

**₹18** 

**₹**19

₹20

₹21 ₹22

₹23

₹40

747

748

749

750

751

752

753

754

755

756

757

758

759

760

761 762

Open Access

**ARTICLE** 

THS, the confluence of semiguinones and metals likely led 63 HO<sub>x</sub>-driven oxidative action within THS films.

Evidence for autoxidation was present in the THS+SQ samp 7656 The present study corroborates prior SQ oxidation stud 67 performed with complementary types of experiments. 768 Analysis of HRMS and MS/MS data suggested that the SQ+7269 Peak 3 was indicative of a compound with multiple site ₹ ₹ ₹ ₹ € € oxidation on the same molecule. Installation of oxidi  $\overline{\mathbf{Z}}$ functional groups at multiple sites on SQ, as suggested by p272 3, could be supported by hydroperoxide decomposition in 7/13 SQ film environment, and/or that peroxides or peracids may 754

active condensed phase oxidants within THS films in addition 765

The impact of persistent autoxidation in THS-contamina 708 surface films does not appear to be restricted 77/9 transformations of the surface film material. The observation 780pronounced cotinine formation in the TCEP and OA/BES ca281 (no observed in clean glass or BES cases) suggests that reac 782 intermediates formed in association with the surface \$183 oxidation process could be oxidizing nicotine to cotini784 whereas in clean glass and BES cases, nicotine oxidat785 appeared to mainly lead to nicotine 1'-N-oxide formation 786 larger relative increase in nicotine 1'-N-oxides was observed 87 the OA/BES film compared to clean glass. The increased cotin 1888 (and to a lesser extent, N-formylnornicotine) production 7&9 TCEP and OA/BES coated glass compared to clean glass n 390 result from a difference in the identity of the oxidan 791 involved, but may also arise from additional nicotine availa 1992 based on uptake from the gas phase and re-partitioning frama3 other surfaces in the chamber. 794

#### **Environmental Significance**

reactive free radical species.

Indoor surfaces harbor chemical films that develop based on the uptake of gaseous and particulate material; 1,4,5 they act **397** reservoir for semivolatile organic compounds, along w198 inorganic acids and bases. 17,18 Recent studies have 3/99 highlighted that surface films and household dust contain EP800 and ROS, 31,37 but the time-evolution of surface film composited 1 due to the presence of condensed phase oxidants has not b802 thoroughly studied. The findings of the present study highl 268 the dynamic nature of surface film chemical composition up 204 the deposition of cigarette smoke, which is known to posses \$95 inherent oxidative potential.47,70 EPFRs can activate 806 formation of highly reactive oxidants (e.g., hydroxyl radic 297 and some EPFRs have lifetimes of months or longer in ambia 68 atmospheric aerosol particle samples. 71 Aerosol particles tag9 contain EPFRs and become deposited on surfaces co&160 influence the composition of environmental surface fi811 gradually over long timescales, as indicated by Filippi et al. 37 &1.02 also shown in the present study. The co-presence of (meta8123) redox couples (e.g., Fe<sup>2+</sup>/Fe<sup>3+</sup>) with EPFRs could lead to the formation of highly reactive (short-lived) oxidants in the condensed phase with subsequent regeneration of EPAR species.<sup>72</sup> Cyclic mechanisms for ROS production would support

the prolonged presence of EPFRs, all the while consistently producing more highly reactive species 9 that 10 and 10 and 10 and 10 and 10 are surface film composition.

**Journal Name** 

The ability of deposits formed by other types of aerosol particles that typically exhibit OP,73 such as biomass burning (BB),33,36 traffic related air pollutants (TRAP),<sup>32</sup> mineral dust,<sup>74</sup> or secondary organic aerosol (SOA),75 to introduce the degree of oxidation chemistry that was conferred by THS in the present study is not yet known, but is likely. It is important to bear in mind that OP assays may respond differently from one another based on the exact nature of the (bio)chemical processes involved in the assay readout,73 so one must retain a critical eye when attempting to predict surface oxidation chemistry using OP assay results. Tobacco smoke could be considered a subset of BB smoke and some assays indicate similar OP.73 Wong et al.<sup>33</sup> showed that atmospheric aging of BB aerosol particles can increase their oxidative potential, so aged or ambient BB aerosol may have more pronounced effects than lab-generated fresh BB. Similarities between THS and TRAP composition polycyclic aromatic compounds and metals,<sup>76</sup> suggesting that TRAP reactivity upon surface deposition could be similar to what has been demonstrated in the present study of THS deposits. In fact, SQ oxidation has been demonstrated in solutions containing metals and PAHs that were meant to serve as a proxy for exposure to urban pollutants.<sup>69</sup> The surface substrate composition may also play a role in driving condensed phase oxidation of surface films, especially if the substrate can provide ingredients for catalytic oxidation, such as Fe2+/Fe3+ or Cu<sup>+</sup>/Cu<sup>2+</sup>. Recent indoor measurements of EPFRs on surfaces strongly suggest that reactivity in films have strong potential,<sup>37</sup> and the delivery of key reactive components might be critical in driving the overall rate of surface film oxidation.

#### Conclusions

795

The effects of cigarette smoking on the indoor environment are continuing to be clarified. Environmental tobacco smoke and second-hand smoke effects are relatively well established, while the importance of THS is still being investigated. The present study provides information on the chemically dynamic nature of THS films over week-long timescales resulting from oxidative transformations of chemicals found in THS and those that may co-exist on indoor surfaces with cigarette smoke residue. The formation of oxidized tobacco alkaloids along with oxidation products of alkenes found on surfaces demonstrates the ability of THS to transform the composition of contaminated indoor surfaces over time. The exact chemical outcomes of THSdriven reactive transformations within real indoor surface films will result from time-dependent behaviour in concert with (and in competition with) bidirectional gas/surface partitioning processes already known to be important for THS and indoor environments more generally.

#### **Author Contributions**

Journal Name ARTICLE

870

871

883

884

885

894

895

815 The authors, AMH and DBC, shared a variety of roles (based 61) 816 the CRediT taxonomy) in the present study, including for analysis, methodology, data curation, conceptualization 817 validation, visualization, writing, and editing. AMH performed 818 most of the investigations. DBC was also responsible for funding 819 acquisition, project administration, resources, and supervision. 820 867 **Conflicts of interest** 868 869 There are no conflicts of interest to declare.

### **Acknowledgements**

<del>8</del>23

824

\$25

**§**26

827

828

₹29

₹30

831

832

**8**33

834

**8**35

**8**36

837

**8**38

₩39

₹40

**8**41

842

848

849

850

13

2024. Downloaded on 2/5/2024 6:27:17 PM.

Open Access Article. Published on 05 February

This project was supported by a grant from the Alfred P. SI&763 Foundation (G-2019-12365) through the SURF-CIE Consort 1764 (via the University of California, San Diego) and the Office of 1879 Provost at Bucknell University. Support was provided by 1870 National Science Foundation for instrumentation (CHE/MRI-2018547), the Physical Sciences Scholars program at Bucknell (DUE/S-STEM-1742124), and the STEM Scholars program at Bucknell (DUE/STEP-1317446). The authors acknowledge the operational support for instrumentation from Dr. Morgan Olse and Dr. Peter Findeis. Maggie E. Young and Naomi R. Dolse assisted with executing some investigations.

#### References

- 886 1 C. M. A. Eichler, J. Cao, G. Isaacman-VanWertz and 87 C. Little, *Indoor Air*, 2019, **29**, 17–29.
- 2 C. J. Weschler and W. W. Nazaroff, *Indoor Air*, 201789
   27, 1101–1112.
- 3 Q.-T. Liu, R. Chen, B. E. McCarry, M. L. Diamond and B91 B. Bahavar, *Environ. Sci. Technol.*, 2003, **37**, 2340–892 2349.
- 4 C. Y. Lim and J. P. Abbatt, *Environ. Sci. Technol.*, 2020, **54**, 14372–14379.
- 5 V. W. Or, M. Wade, S. Patel, M. R. Alves, D. Kim, S<sub>896</sub> Schwab, H. Przelomski, R. O'Brien, D. Rim, R. L. Cossi, M. E. Vance, D. K. Farmer and V. H. Grassian, 898 Environ. Sci.: Processes Impacts, 2020, **22**, 1698–899 1709.
- 851 6 P. Jacob, N. L. Benowitz, H. Destaillats, L. Gundel, \(\beta\_{01}\)
  852 Hang, M. Martins-Green, G. E. Matt, P. J. E. 902
  853 Quintana, J. M. Samet, S. F. Schick, P. Talbot, N. J. 903
  854 Aquilina, M. F. Hovell, J.-H. Mao and T. P. 904
  855 Whitehead, Chem. Res. Toxicol., 2017, 30, 270–29\(\delta\_{05}\)
- 856 7 A. P. Ault, V. H. Grassian, N. Carslaw, D. B. Collins, 66 857 Destaillats, D. J. Donaldson, D. K. Farmer, J. L. 907
- Jimenez, V. F. McNeill, G. C. Morrison, R. E. O'Brieg<sub>08</sub>
  M. Shiraiwa, M. E. Vance, J. R. Wells and W. Xiong<sub>909</sub>
- 860 *Chem*, 2020, **6**, 3203–3218.

- 8 R. E. O'Brien, Y. Li, K. J. Kiland, E. F. Katz, Vie Min Qron Ene Legaard, E. Q. Walhout, C. Thrasher, V. 143 Grassian, P. F. DeCarlo, A. K. Bertram and M. Shiraiwa, Environ. Sci.-Process Impacts, 2021, 23, 559–568.
- 9 M. L. Diamond, S. E. Gingrich, K. Fertuck, B. E. McCarry, G. A. Stern, B. Billeck, B. Grift, D. Brooker and T. D. Yager, *Environ. Sci. Technol.*, 2000, **34**, 2900–2908.
- 10 J. S. Grant, Z. Zhu, C. R. Anderton and S. K. Shaw, *ACS Earth Space Chem.*, 2019, **3**, 305–313.
- 11 D. B. Collins and V. H. Grassian, in *Physical Chemistry* of Gas-Liquid Interfaces, Elsevier, 2018, pp. 271–313.
- 12 U. Pöschl and M. Shiraiwa, *Chemical Reviews*, 2015, **115**, 4440–4475.
- 13 R. Habre, D. C. Dorman, J. Abbatt, W. P. Bahnfleth, E. Carter, D. Farmer, G. Gawne-Mittelstaedt, A. H. Goldstein, V. H. Grassian, G. Morrison, J. Peccia, D. Poppendieck, K. A. Prather, M. Shiraiwa, H. M. Stapleton, M. Williams and M. E. Harries, *Environ. Sci. Technol.*, 2022, **56**, 10560–10563.
- 14 V. Bahl, P. J. Iii, C. Havel, S. F. Schick and P. Talbot, *PLOS ONE*, 2014, **9**, e108258.
- 15 G. Morrison, *Environ. Sci. Technol.*, 2008, **42**, 3495–3499.
- 16 M. Sleiman, J. M. Logue, W. Luo, J. F. Pankow, L. A. Gundel and H. Destaillats, *Environ. Sci. Technol.*, 2014, **48**, 13093–13101.
- 17 D. M. Lunderberg, K. Kristensen, Y. Tian, C. Arata, P. K. Misztal, Y. Liu, N. Kreisberg, E. F. Katz, P. F. DeCarlo, S. Patel, M. E. Vance, W. W. Nazaroff and A. H. Goldstein, *Environ. Sci. Technol.*, 2020, **54**, 6751–6760.
- 18 C. Wang, D. B. Collins, C. Arata, A. H. Goldstein, J. M. Mattila, D. K. Farmer, L. Ampollini, P. F. DeCarlo, A. Novoselac, M. E. Vance, W. W. Nazaroff and J. P. D. Abbatt, *Science Advances*, 2020, **6**, eaay8973.
- 19 D. B. Collins, C. Wang and J. P. D. Abbatt, *Environ. Sci. Technol.*, 2018, **52**, 13195–13201.
- 20 P. F. DeCarlo, A. M. Avery and M. S. Waring, *Science Advances*, 2018, **4**, eaap8368.
- 21 I. J. George and J. P. D. Abbatt, *Nature Chem*, 2010, **2**, 713–722.
- 22 M. Shiraiwa, Y. Sosedova, A. Rouvière, H. Yang, Y. Zhang, J. P. D. Abbatt, M. Ammann and U. Pöschl, *Nature Chemistry*, 2011, **3**, 291–295.
- 23 T. Berkemeier, A. Mishra, C. Mattei, A. J. Huisman, U. K. Krieger and U. Pöschl, *ACS Earth Space Chem.*, 2021, **5**, 3313–3323.
- 24 T. Nah, S. H. Kessler, K. E. Daumit, J. H. Kroll, S. R. Leone and K. R. Wilson, *Phys. Chem. Chem. Phys.*, 2013, **15**, 18649.

910

<u>9</u>20

**9**21

₫22

<u>\$</u>29

₹30

**9**31

**§**32

**9**33

**∮**34

**9**35

**9**36

₫37

**9**38

<del>§</del>39

<u>9</u>40

941

<u>ğ</u>42

13

15

16

948 949

950

Open Access

Article. Published on 05 February 2024. Downloaded on 2/5/2024 6:27:17 PM.

ARTICLE Journal Name

| 912 | 25 L. M. Petrick, M. Sleiman, Y. Dubowski, L. A. Gund <b>9</b> 62 |
|-----|---|
| 913 | and H. Destaillats, Atmospheric Environment, 2019,63              |
| 914 | <b>45</b> , 4959–4965. 964  |

- 915 26 X. Tang, N. R. González, M. L. Russell, R. L.
  965
  916 Maddalena, L. A. Gundel and H. Destaillats,
  966
- 917 Environmental Research, 2020, 110462.
- 918 27 R. Alwarda, S. Zhou and J. P. D. Abbatt, *Indoor Air*,968 919 2018, **28**, 655–664. 969
  - 28 J. D. Crounse, L. B. Nielsen, S. Jørgensen, H. G. 970 Kjaergaard and P. O. Wennberg, *J. Phys. Chem. Le***27**,1 2013, **4**, 3513–3520. 972
- \$23
   \$29 F. Bianchi, T. Kurtén, M. Riva, C. Mohr, M. P.
   \$24
   \$24
   \$25
   \$25
   \$25
   \$26
   \$27
   \$28
   \$28
   \$29
   \$29
   \$20
   \$20
   \$20
   \$20
   \$20
   \$20
   \$20
   \$20
   \$20
   \$20
   \$20
   \$20
   \$20
   \$20
   \$20
   \$20
   \$20
   \$20
   \$20
   \$20
   \$20
   \$20
   \$20
   \$20
   \$20
   \$20
   \$20
   \$20
   \$20
   \$20
   \$20
   \$20
   \$20
   \$20
   \$20
   \$20
   \$20
   \$20
   \$20
   \$20
   \$20
   \$20
   \$20
   \$20
   \$20
   \$20
   \$20
   \$20
   \$20
   \$20
   \$20
   \$20
   \$20
   \$20
   \$20
   \$20
   \$20
   \$20
   \$20
   \$20
   \$20
   \$20
   \$20
   \$20
   \$20
   \$20
   \$20
   \$20
   \$20
   \$20
   \$20
   \$20
   \$20
   \$20
   \$20
   \$20
   \$20
   \$20
   \$20
   \$20
   \$20
   \$20
   \$20
   \$20
   \$20
   \$20
   \$20
   \$20
   \$20
   \$20
   \$20
   \$20
   \$20
   \$20
   \$20
   \$20
   \$20
   \$20
   \$20
   \$20
   \$20
   \$20
   \$20
   \$20
   <
  - 30 T. Berkemeier, S. S. Steimer, U. K. Krieger, T. Peter979 U. Pöschl, M. Ammann and M. Shiraiwa, *Phys. Ch***98**0 *Chem. Phys.*, 2016, **18**, 12662–12674. 981
  - 31 G. Morrison, R. Moravec and Z. Yao, *Environ. Sci.* 982 *Technol. Lett.*, , DOI:10.1021/acs.estlett.3c00290. 983
  - 32 S. Biswas, V. Verma, J. J. Schauer, F. R. Cassee, A. 1984 Cho and C. Sioutas, *Environ. Sci. Technol.*, 2009, **43**,85 3905–3912. 986
  - 33 J. P. S. Wong, M. Tsagkaraki, I. Tsiodra, N. 987 Mihalopoulos, K. Violaki, M. Kanakidou, J. Sciare, A88 Nenes and R. J. Weber, *Environ. Sci. Technol.*, 201**9**89 **53**, 6747–6756. 990
  - 34 A. Valavanidis, T. Vlachogianni and K. Fiotakis, *Int* 991 *Environ Res Public Health*, 2009, **6**, 445–462. 992
  - 35 J. G. Charrier and C. Anastasio, *Atmospheric* 993 *Chemistry and Physics*, 2012, **12**, 9321–9333. 994
  - 36 W. Y. Tuet, F. Liu, N. de Oliveira Alves, S. Fok, P. 995 Artaxo, P. Vasconcellos, J. A. Champion and N. L. 1996 Environ. Sci. Technol. Lett., 2019, 6, 126–132. 997
  - 37 A. Filippi, R. Sheu, T. Berkemeier, U. Pöschl, H. Tor 998 and D. R. Gentner, *Environ. Sci.: Atmos.*, 2022, **2**, 999 128–136.
- 951 38 S. F. Schick, K. F. Farraro, C. Perrino, M. Sleiman, 13001
   952 van de Vossenberg, M. P. Trinh, S. K. Hammond, 18002
   953 M. Jenkins and J. Balmes, *Tobacco Control*, 2014, 128, 3
   954 152–159. 1004
- 39 M. Sleiman, L. A. Gundel, J. F. Pankow, P. Jacob, **B.00**5
   Singer and H. Destaillats, *Proc Natl Acad Sci USA*,1006
   2010, **107**, 6576–6581.
- 958 40 G. E. Matt, P. J. E. Quintana, M. F. Hovell, J. T. 1008 959 Bernert, S. Song, N. Novianti, T. Juarez, J. Floro, Cl009
- 960 Gehrman, M. Garcia and S. Larson, *Tob Control*, 1010
   961 2004, 13, 29. 1011

- 41 G. E. Matt, A. L. Merianos, P. J. E. Quintana, Erithohiine N. G. Dodder and E. M. Mahabee-Gittlens, JAMA <sup>0142C</sup> Network Open, 2022, **5**, e2147184.
- 42 A. Wylie, University of Toronto, 2020.
- 43 R. Sheu, C. Stönner, J. C. Ditto, T. Klüpfel, J. Williams and D. R. Gentner, *Science Advances*, 2020, **6**, eaay4109.
- 44 R. Sheu, T. Hass-Mitchell, A. Ringsdorf, T. Berkemeier, J. Machesky, A. Edtbauer, T. Klüpfel, A. Filippi, B. A. M. Bandowe, M. Wietzoreck, P. Kukučka, H. Tong, G. Lammel, U. Pöschl, J. Williams and D. R. Gentner, *Environ. Sci.: Atmos.*, , DOI:10.1039/D1EA00107H.
- 45 K. Yeh, L. Li, F. Wania and J. P. D. Abbatt, Environment International, 2022, **160**, 107063.
- 46 A. Rodgman and T. A. Perfetti, *The Chemical Components of Tobacco and Tobacco Smoke*, CRC Press, Boca Raton, FL, Second Edition., 2013.
- 47 D. F. Church and W. A. Pryor, *Environmental Health Perspectives*, 1985, **64**, 111–126.
- 48 M. Shein and G. Jeschke, *Chem Res Toxicol*, 2019, **32**, 1289–1298.
- 49 J. B. Wooten, S. Chouchane and T. E. McGrath, in *Cigarette Smoke and Oxidative Stress*, eds. B. Halliwell and H. E. Poulsen, Springer, Berlin, 2006, pp. 5–46.
- 50 M. Egawa, Y. Kohno and Y. Kumano, *International Journal of Cosmetic Science*, 1999, **21**, 83–98.
- 51 Q. Zhang, S. Tang, G. Huang and H. Liu, *Journal of Cosmetic Dermatology*, 2022, **21**, 3085–3094.
- 52 G. Percoco, A. Patatian, F. Eudier, M. Grisel, T. Bader, E. Lati, G. Savary, C. Picard and P. Benech, *Experimental Dermatology*, 2021, **30**, 1610–1618.
- 53 B. L. Deming and P. J. Ziemann, *Indoor Air*, 2020, **30**, 914–924.
- 54 B. X. MacLean, B. S. Pratt, J. D. Egertson, M. J. MacCoss, R. D. Smith and E. S. Baker, *J. Am. Soc. Mass Spectrom.*, 2018, **29**, 2182–2188.
- 55 K. J. Adams, B. Pratt, N. Bose, L. G. Dubois, L. St John-Williams, K. M. Perrott, K. Ky, P. Kapahi, V. Sharma, M. J. MacCoss, M. A. Moseley, C. A. Colton, B. X. MacLean, B. Schilling, J. W. Thompson, and Alzheimer's Disease Metabolomics Consortium, *J Proteome Res*, 2020, 19, 1447–1458.
- 56 T. J. Smyth, V. N. Ramachandran, A. McGuigan, J. Hopps and W. F. Smyth, *Rapid Communications in Mass Spectrometry*, 2007, **21**, 557–566.
- 57 P. Jacob, M. L. Goniewicz, C. M. Havel, S. F. Schick and N. L. Benowitz, *Chem. Res. Toxicol.*, 2013, **26**, 1615–1631.

**Journal Name ARTICLE** 

> View Article Online DOI: 10.1039/D3EA00142C

- 1012 58 N. J. Aquilina, C. M. Havel, P. Cheung, R. M. Harrison,
- 1013 K.-F. Ho, N. L. Benowitz and P. Jacob III, Environment
- 1014 International, 2021, **150**, 106417.
- 59 P. A. Crooks, in *Nicotine and Related Alkaloids*, eds. 1015
- 1016 J. W. Gorrod and J. Wahren, 1993, pp. 81–109.
- 1017 60 S. Zhou, B. C. H. Hwang, P. S. J. Lakey, A. Zuend, J. P.
- 1018 D. Abbatt and M. Shiraiwa, PNAS, 2019, 116, 11658-**101**9 11663.
- 1\frac{1}{2}0 61 Z. Zhou, S. Zhou and J. P. D. Abbatt, Environ. Sci.
- 1021 Technol., 2019, 53, 12467-12475.
- 1 62 M. Shiraiwa, M. Ammann, T. Koop and U. Pöschl,
- 1**2**23 Proceedings of the National Academy of Sciences, ≥1**0**24
- 2011, **108**, 11003-11008. **⊆1**825

ട**1₫37** 

<u>-</u>51₿38

ອ**10**41 1<u>0</u>42

15

<del>104</del>8

1049

- 63 E. Camera, M. Ludovici, M. Galante, J.-L. Sinagra and **5**1**6**26 M. Picardo, Journal of Lipid Research, 2010, 51, 3377-3388.
- )41<u>0</u>27/2/07 1<u>0</u>28 1<u>0</u>28 1<u>0</u>29 64 K. A. Mountfort, H. Bronstein, N. Archer and S. M. Jickells, Anal. Chem., 2007, 79, 2650-2657. pp1030 1031 1032 1032
  - 65 K. Nakagawa, D. Ibusuki, Y. Suzuki, S. Yamashita, O. Higuchi, S. Oikawa and T. Miyazawa, Journal of Lipid Research, 2007, 48, 2779–2787.
  - 66 B. N. Dorakumbura, F. Busetti and S. W. Lewis, 31.
- 1033 201033 67 N. Shimizu, H. Bersabe, J. Ito, S. Kato, R. Towada, T. ទ្ឋិវម្ជី35 Eitsuka, S. Kuwahara, T. Miyazawa and K. Nakagawa, <sub>2</sub>51**9**36 J. Oleo Sci., 2017, 66, 227-234.
  - 68 N. Shimizu, J. Ito, S. Kato, Y. Otoki, M. Goto, T. Eitsuka, T. Miyazawa and K. Nakagawa, Sci Rep, 2018, 8, 9116.
  - 69 F. Eudier, N. Hucher, C. Picard, G. Savary and M. Grisel, Chem. Res. Toxicol., 2019, 32, 285-293.
  - 70 W. A. Pryor, B. J. Hales, P. I. Premovic and D. F. Church, Science, 1983, 220, 425-427.
  - 71 W. Gehling and B. Dellinger, Environ Sci Technol, 2013, **47**, 8172–8178.
  - 72 R. Chen and J. J. Pignatello, Environ. Sci. Technol., 1997, 31, 2399-2406.
  - 73 H. J. Forman and C. E. Finch, Free Radical Biology and Medicine, 2018, 117, 202-217.
  - 1050 74 C. Nishita-Hara, H. Kobayashi, K. Hara and M.
  - 1051 Hayashi, GeoHealth, 2023, 7, e2022GH000736. 1052
  - 75 W. Y. Tuet, Y. Chen, L. Xu, S. Fok, D. Gao, R. J. Weber 1053 and N. L. Ng, Atmospheric Chemistry and Physics, 1054 2017, **17**, 839–853.
  - 1055 76 G. C. Lough, J. J. Schauer, J.-S. Park, M. M. Shafer, J.
  - 1056 T. DeMinter and J. P. Weinstein, Environ. Sci.
  - 1057 Technol., 2005, 39, 826-836.